



Comparative study of radiation effect on titanium dioxide power-law nanofluid over a thin needle with cancer treatment applications: a quadratic regression model

Palani Sathya¹ · Padigepati Naveen¹

Received: 31 January 2024 / Accepted: 18 March 2024 / Published online: 6 May 2024
© Akadémiai Kiadó, Budapest, Hungary 2024

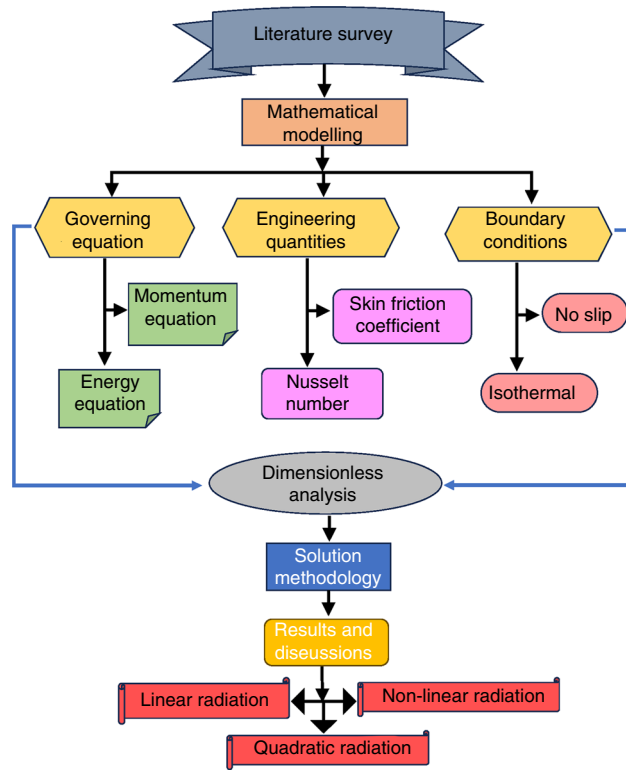
Abstract

Non-Newtonian fluids with nanomaterials are studied to improve industrial efficiency and production by enhancing thermal conductivity. In addition, the titanium dioxide nanoparticles can easily penetrate cells and tissues due to their small size. Its photocatalytic activities can also be utilized to produce reactive oxygen species, which have potential applications in cancer treatment. So, the present investigation intends to analyze the water-based titanium dioxide power-law nanofluid flow over a thin needle. Further, the thermal radiation was incorporated and analyzed as a complete case study for linear, nonlinear, and quadratic radiation. The governing equations are reformed into a dimensionless form using suitable similarity variables. Numerical solutions were found by implementing the Bvp4c technique. The major conclusion drawn from the present investigation reveals that the temperature is enhanced by the radiation, needle size, and titanium dioxide volume fraction. The nonlinear radiation case plays a dominant role compared to the other two radiation cases. In order to provide further insight into the engineering quantities, multiple quadratic regression models are utilized to predict skin friction and thermal transmission rate. The quadratic regression term of radiation and temperature ratio parameters has a negative influence on the heat transmission rate. The outcomes of this investigation may help to get a better theoretical understanding of various scientific research and biomedical applications, especially in the treatment of tumors, sterilization of medical instruments, drug delivery systems, and cancer treatment.

✉ Padigepati Naveen
naveenpadi09@gmail.com

¹ Department of Mathematics, School of Advanced Sciences, Vellore Institute of Technology, Vellore, Tamil Nadu 632014, India

Graphical abstract



Keywords Power-law nanofluid · Titanium dioxide nanoparticles · Radiation case study · Thin needle · Regression analysis

List of symbols

a	Needle thickness
C_f	Surface drag coefficient (skin friction) $\frac{2\tau_w}{\rho U^2}$
C_p	Specific heat capacitance [$\text{J kg}^{-1} \text{K}^{-1}$]
f	Dimensionless stream function
k_f	Thermal conductivity [$\text{kg m K}^{-1} \text{s}^{-3}$]
k^*	Radiation absorption coefficient (m^{-1})
l	Characteristic length (m)
n	Non-Newtonian fluid power-law index
Nu_1	Heat transfer rate (local Nusselt number), $\frac{xq_w}{k_f(T_w - T_\infty)}$
Pr	Generalized Prandtl number, $\frac{Ul}{\alpha_f} \left(Re_1 \right)^{\frac{-2}{n+1}}$
q_w	Heat flux at needle surface
q_{rad}	Radiative heat flux [$\text{kg m}^{-1} \text{s}^{-3} \text{K}^{-1}$]
Re_1	Reynolds number, $\frac{U^{2-n} l^n}{v_f}$
Rd	Radiation parameter, $\frac{4\sigma^* T_\infty^3}{k_f k^*}$
R	Needle radius (m)
T	Temperature of fluid (K)
T_w	Surface temperature at plate (K)
T_∞	Ambient temperature (K)

u Velocity of fluid in x (directional axis) direction (m/s)
 v Velocity of fluid in r (radial axis) direction (m/s)

Greek symbols

η	Similarity variable
ρ	Fluid density (kg m^{-3})
σ^*	Stefan–Boltzmann constant ($\text{kg s}^{-3} \text{K}^{-4}$)
τ_w	Shear stress at needle surface
θ	Dimensionless temperature
θ_{tr}	Temperature ratio parameter, $\frac{T_w}{T_\infty}$
ψ	Stream function

Subscripts

f	Denotes for base fluid
nf	Denotes for nanofluid
w	Denotes conditions at needle surface
∞	Denotes ambient medium conditions

Introduction

Non-Newtonian fluids [1, 2] have an extensive range of potential applications over ten years in numerous industrial and engineering domains. One of the most widely utilized non-Newtonian models is the power-law fluid. This fluid models are utilized in the biomedical industries to handle the viscosity of different formulations such as the efficient circulation of blood flow through vessels, suspensions, and gels. Similarly, it helps in pharmaceutical products such as ointments, lotion, and drug suspension to control the fluid viscosity and improve the spread-ability and stability. Comprehending the rheology behavior of these liquids is crucial to ensure a consistent and reliable drug delivery system. Recently, Bahmani et al. [3] studied the natural convection of power-law fluids over a horizontally heated plate. Later, the study of heat transmission of power-law fluid flow along a circular cylinder was investigated by Parvez et al. [4]. Moreover, some researchers [5–7] have made use of this model to examine the boundary layer flow over different geometry by taking various flow circumstances into account because of its extensive range of applications.

Due to its potential applications, nanofluid [8] could be an innovative coolant for the automotive industry. It efficiently combines liquid, air, and two-phase cooling to remove excessive heat flux in electronic appliances [9, 10]. Moreover, a lot of research works [11–14] provide substantial research on nanofluids and their physical significance. Especially in biomedical industries [15], it is also beneficial in drug delivery and cancer imaging for cancer therapeutics. However, this study mainly focuses on biomedical applications, especially in cancer treatment and drug delivery. This study has chosen titanium dioxide as its nanoparticle. Some existing experimental results [16, 17] reveal that titanium dioxide (TiO_2) particles have a potential application in the biomedical field, particularly in treating tumors, cancer, sonodynamic therapy (SDT), photodynamic therapy (PDT), and drug delivery systems. Innovative therapies and treatments will be developed as long as cancer affects people, and researchers will use nanotechnology as a key tool to achieve this goal [18].

The energy emitted as electromagnetic waves by objects that are hotter than zero or absolute zero is termed thermal radiation. These heat waves can penetrate up to two inches into muscle and tissue. Further, it is most effective for injuries to the tendons, muscles, and joints. Furthermore, recent research has shown that hyperthermia can be a successful treatment during cancer treatments [19]. This process aims to bring the infected tissues up to $45^\circ C$, above the cytotoxic temperature of $41^\circ C$, without causing excessive damage stress to healthy cells. The linear radiation by Rosseland approximation is commonly applied in many technical processes. However, linear radiation is no longer adequate

[20] due to higher temperature differences and density temperature variation in many practical situations such as thermal equipment, chemical combustion, and energy storage facilities. Therefore, this investigation focuses on analyzing the complete comparative analysis for radiation heat transmission such as linear, nonlinear, and quadratic radiation. Recently, Mahanthesh et al. [21] revealed that the nonlinear radiation case plays a dominant role compared to other cases in the study of the quadratic flow of nanofluid along a vertical plate. Later, Sneha et al. [22] found that enhancing radiation parameter upsurges the temperature profile in the study of radiation effects on the Casson nanofluid in the presence of chemical reaction. A significant number of investigations [23–25] studies on linear, quadratic, and nonlinear radiation have been carried out recently due to their potential application.

In addition, the utilization of titanium dioxide nanoparticles as an enhancing agent in radiation therapy and computed tomography imaging (CT) has been studied by Smith et al. [26]. Ionizing radiation targets tumors and damages tumor cells' DNA, causing the cells to die. This process is known as radiation treatment.

Recently, numerous researchers have seized the opportunity to analyze the study of axisymmetric boundary layer flow and heat transmission induced by thin needles in different fluids due to its several technological applications. A thin needle is a slandering object with a parabolic revolution around an axis. In experimental studies for flow and heat transfer analysis, the main focus is on the situation where the thin needle's motion distracts from the free stream direction, making it possible to measure the system's temperature and velocity profiles. A few prominent uses for thin needle technology include heated wire anemometers in wind technology, microcooling systems for heat removal, aerodynamics, infinitesimal equipment, metal spinning, and other micro-electronic devices. Specifically in the biomedical field, it is utilized in cancer treatment, drug delivery, and blood flow problems. Initially, Lee [27] presented the development of a boundary layer in the viscous fluid adjacent to a thin needle. Recently, Hassan et al. [28] investigated the heat transmission rate of non-Newtonian nanofluid's flow along a thin needle employing experimental data-based mathematical methodology. Moreover, many researchers [29–31] have presented their investigation on boundary layer flow over thin needles with various fluid models and different situations.

Based on the existing literature, it is evident that, to the author's best knowledge, no attempts have been made thus far to investigate power-law nanofluid flow over a thin needle subject to radiation effects. The present investigation intends to analyze the power-law nanofluid flow over a thin needle. In addition to that, the complete case studies of linear, nonlinear, and quadratic thermal radiation are incorporated. The governing equations are altered into the dimensionless form

utilizing suitable similarity variables. Numerical solutions are found by implementing the Bvp4c technique. The findings are thoroughly examined and visualized graphically. In order to provide further insight into the engineering quantities, multiple quadratic regression models are utilized to predict surface drag force and thermal transmission rate. The subsequent question provides more insight into the significance of this investigation.

- How does the radiation effects on the temperature profile?
- Which radiation case plays a dominant role in the thermal distribution?
- Will the needle thickness and TiO_2 volume fraction influence the flow field or not?
- What are the advantages of TiO_2 nanoparticles with radiation in destroying cancer cells?
- In the flow field, which fluid case of the power-law fluid is dominant?
- In linear and quadratic models, which regression model gives more accurate results?

The answers to these questions may help to get a better theoretical understanding of various scientific research and biomedical applications, especially in the treatment of tumors, sterilization of medical instruments, and cancer treatment.

Mathematical model

Consider the time-independent axisymmetric flow of power-law nanofluid over a thin needle of radius R . Assuming (x, r) cylindrical coordinates, this gives us x as the directional axis with the radial axis, r as its normal, and a as the needle thickness ($a \neq 0$). The flow geometry is visualized in Fig. 1. In addition, we assume the following assumptions [27]:

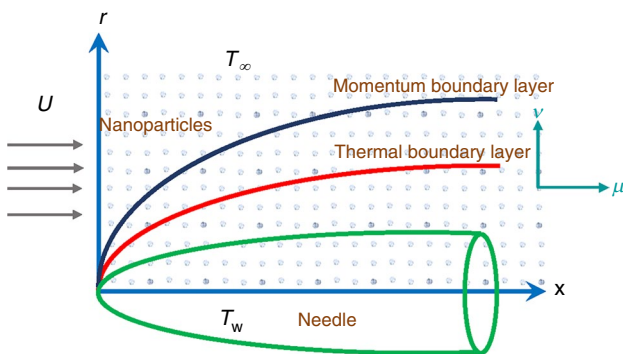


Fig. 1 Flow geometry of the current problem

- The surface and ambient temperature are taken as T_w and T_∞ .
- The pressure gradient along the surface of the needle is negligible.
- The needle's thickness is comparable to or less than the momentum and thermal boundary layers surrounding it.
- The transverse curvature effect of thin needle is significant.

Based on the assumptions mentioned above, the governing equation (in cylindrical coordinates) is formulated as follows [5, 22, 32]:

$$\frac{\partial u}{\partial x} + \frac{v}{r} + \frac{\partial v}{\partial r} = 0, \quad (1)$$

$$r\rho_{nf}\left(u\frac{\partial u}{\partial x} + v\frac{\partial u}{\partial r}\right) = \frac{\partial}{\partial r}\left[r\mu_{nf}\left(\frac{\partial u}{\partial r}\right)^n\right], \quad (2)$$

$$(\rho c_p)_{nf}\left(u\frac{\partial T}{\partial x} + v\frac{\partial T}{\partial r}\right) = \frac{k_{nf}}{r}\frac{\partial}{\partial r}\left[r\frac{\partial T}{\partial r}\right] - \frac{1}{r}\frac{\partial(rq_{rad})}{\partial r}, \quad (3)$$

where T is the temperature of the fluid and (u, v) are the velocity components of (x, r) direction, respectively. The index n indicates the flow behavior with shear thinning ($n < 1$), Newtonian ($n = 1$), and shear thickening fluid ($n > 1$) cases, respectively. The last term of the energy equation is the heat flux due to radiation (q_{rad}). Here, $(\rho)_{nf}$, $(k)_{nf}$, $(\rho C_p)_{nf}$ and $(\mu)_{nf}$ are effective density, thermal conductivity, heat capacitance, and dynamic viscosity of the nanofluid, respectively.

For this flow configuration, the feasible surface conditions are free stream conditions of the boundary layer's edge and no-slip effect which are stated at the needle's surface ($r = R$) as follows [5]:

$$u(R) = 0, \quad v(R) = 0, \quad u(\infty) = U, \quad T(R) = T_w, \quad T(\infty) = T_\infty. \quad (4)$$

Radiation case study

Rosseland approximation is utilized to express the heat flux due to radiation in the energy equation which enhances the efficiency of numerous thermal transport systems. It plays an essential role in the treatment of tumors, sterilization of medical instruments, and cancer treatment. Assume that the fluid is optically thick. The Rosseland approximation is expressed as follows [22, 33]:

$$q_{rad} = \frac{-4\sigma^*}{3k^*} \frac{\partial T^4}{\partial r}$$

where k^* and σ^* symbolize the mean absorption coefficient and the Stefan–Boltzmann constant, respectively.

By incorporating Taylor's series, the expansion of T^4 is

$$T^4 \approx T_\infty^4 + 4T_\infty^3(T - T_\infty) + 6T_\infty^2(T - T_\infty)^2 + \dots, \quad (5)$$

Higher-order terms are negligible when the temperature variation is small. Hence, it is appropriate to incorporate the heat flux due to linear radiation as follows [25]:

$$\begin{aligned} T^4 &\approx 4T_\infty^3 T - 3T_\infty^4 \\ q_{\text{rad}} &= \frac{-16\sigma^* T_\infty^3}{3k^*} \frac{\partial T}{\partial r}. \end{aligned} \quad (6)$$

This case is no longer adequate when the temperature difference is extremely high. So, the heat flux due to nonlinear radiation is more suitable to incorporate which is expressed as follows [34, 35],

$$q_{\text{rad}} = \frac{-16\sigma^* T^3}{3k^*} \frac{\partial T}{\partial r}, \quad (7)$$

Similarly, the quadratic approximation is appropriate to consider for sufficiently large density-temperature variations since it significantly affects heat transport. Then, the series is truncated after the quadratic term.

$$T^4 \approx 3T_\infty^4 - 8T_\infty^3 T + 6T_\infty^2 T^2$$

The heat flux due to quadratic radiation is expressed as follows: [22]

$$q_{\text{rad}} = \frac{-4\sigma^* T^3}{3k^*} \left(-8T_\infty^3 \frac{\partial T}{\partial r} + 12T_\infty^2 T \frac{\partial T}{\partial r} \right). \quad (8)$$

Finally, Eqs. (6), (7), and (8) are implemented in Eq. (3) for the computation of radiative heat flux for linear, nonlinear, and quadratic radiation cases, respectively.

Dimensionless analysis

The similarity variable [5] for the present investigation is expressed as follows:

$$\eta = r \left(\frac{x}{b} \right)^{-m}, \theta = \frac{(T - T_\infty)}{(T_w - T_\infty)}, \quad (9)$$

where $m = (n + 1)^{-1}$ and $b = \frac{2m}{v_f U^{n-2}}$. Additionally, it should be observed that the constant values of $\eta \neq 0$ symbolize the surfaces of revolution (ranges from a to ∞) and that $\eta = a$ yields the needle's surface, which is expressed as follows:

$$\eta = R \left(\frac{x}{b} \right)^{-m} = a$$

A stream function f can be introduced conveniently, and the velocity components u and v can be expressed as follows:

$$\frac{u}{U} = 2f + \eta f'; \quad \frac{v}{U} = mb^{-m} x^{m-1} \eta^2 f'; \quad (10)$$

By implementing the transformation (9)–(10) under the consideration of (6)–(8), the governing equation (2)–(4) reduced as follows:

$$nf''' + \frac{4n+1}{\eta} f'' + \frac{3}{\eta^2} f' + \frac{A_2}{A_1} [3f' + \eta f'']^{2-n} f = 0 \quad (11)$$

Linear Case:

$$\begin{aligned} &\left(A_3 + \frac{4}{3} Rd \right) \theta'' \\ &+ \left[2A_4 f m \eta (2m)^{-2m} (x^*)^{\frac{1-n}{1+n}} Pr + \frac{A_3}{\eta} + \frac{4}{3} \eta Rd \right] \theta' = 0 \end{aligned} \quad (12)$$

Nonlinear Case:

$$\begin{aligned} &\left(1 + \frac{4}{3A_3} Rd \{ 1 + [\theta_{\text{tr}} - 1] \theta \}^3 \right) \left[\frac{\theta'}{\eta} + \theta'' \right] \\ &+ 2 \frac{A_4}{A_3} m (2m)^{-2m} (x^*)^{\frac{1-n}{1+n}} Pr f \theta' \eta \\ &+ \frac{4Rd}{A_3} (\theta_{\text{tr}} - 1) \{ 1 + (\theta_{\text{tr}} - 1) \theta \}^2 (\theta')^2 = 0 \end{aligned} \quad (13)$$

Quadratic Case:

$$\begin{aligned} &\left(1 + \frac{4Rd}{3A_3} [3\{ 1 + (\theta_{\text{tr}} - 1) \theta \} - 2] \right) \left(\frac{\theta'}{\eta} + \theta'' \right) \\ &+ 2 \frac{A_4}{A_3} f \theta' m \eta (2m)^{-2m} (x^*)^{\frac{1-n}{1+n}} Pr \\ &+ \frac{4Rd}{A_3} (\theta_{\text{tr}} - 1) (\theta')^2 = 0 \end{aligned} \quad (14)$$

along with corresponding boundary conditions

$$\begin{aligned} f(\eta) &= f'(\eta) = 0, \quad \theta(\eta) = 1 \text{ as } \eta \rightarrow a \\ f(\eta) &= \frac{1}{2}, \quad \theta(\eta) = 0 \text{ as } \eta \rightarrow \infty \end{aligned} \quad (15)$$

The dimensionless parameters presented in the above equation are radiation parameter, Reynolds number, generalized Prandtl number, and temperature ratio which are expressed as follows:

Table 1 Thermophysical characteristics of water and TiO₂[36, 37]

Properties	Water	TiO ₂
ρ (kg/m ³)	997.1	4250
K (W/mK)	0.613	8.9538
C_p (J/kgK)	4179	686.2

$$\begin{aligned} Rd &= \frac{4\sigma^* T_\infty^3}{k^* k_f}; Re_1 = \frac{U^{2-n} l^n}{v_f}; \\ Pr &= \frac{Ul}{\alpha_f} \left(Re_1^{\frac{-2}{n+1}} \right); \theta_{tr} = \frac{T_w}{T_\infty}; x^* = \frac{x}{l}; \\ A_1 &= \frac{\mu_{nf}}{\mu_f}; A_2 = \frac{\rho_{nf}}{\rho_f}; \\ A_3 &= \frac{K_{nf}}{K_f}; A_4 = \frac{(\rho C_p)_{nf}}{(\rho C_p)_f} \end{aligned} \quad (16)$$

where l is the characteristic needle length and thermophysical terms of nanofluid are [32]:

$$\begin{aligned} \mu_{nf} &= \mu_f(1 - \phi)^{-2.5}; \\ (\rho C_p)_{nf} &= (1 - \phi)(\rho C_p)_f + \phi(\rho C_p)_s \\ \rho_{nf} &= (1 - \phi)\rho_f + \phi\rho_s; \\ k_{nf} &= k_f \left[\frac{(k_s + 2k_f) - 2\phi(k_f - k_s)}{(k_s + 2k_f) + \phi(k_f - k_s)} \right] \end{aligned} \quad (17)$$

The thermophysical properties of water and TiO₂ are displayed in Table 1. Selected TiO₂ particles can easily penetrate cells and tissues due to their small size. Its photocatalytic activities can also be utilized to produce Reactive Oxygen Species (ROS), which have potential applications in cancer treatment [17]. In addition, titanium dioxide nanoparticles are utilized as an enhancing agent in radiation therapy and computed tomography imaging (CT). Moreover, ionizing radiation targets tumors and damages tumor cells' DNA, causing the cells to die. This process is known as radiation treatment[26].

Engineering quantities

The frictional drag coefficient (C_f) which helps to study the drag force at the surface for the present investigation is expressed as

$$C_f = \frac{2\tau_w}{\rho U^2}$$

Similarly, the Nusselt number (Nu_x) which helps to study the rate of thermal transmission is expressed as

$$Nu_x = \frac{x q_w}{k_f(T_w - T_\infty)}$$

By implementing (9)–(10), the dimensionless quantities are follows:

$$Re_x^m C_f = 2A_1(2m)^{mn} (af''(a))^n \quad (18)$$

Linear Case:

$$Re_1^{-m} Nu_x = -(x^*)^{mn} (2m)^m \left[A_3 + \frac{4}{3} Rd \right] \theta'(a) \quad (19)$$

Nonlinear Case:

$$Re_1^{-m} Nu_x = -(x^*)^{mn} (2m)^m \left[A_3 + \frac{4}{3} Rd \{ 1 + (\theta_{tr} - 1)\theta(a) \}^3 \right] \theta'(a) \quad (20)$$

Quadratic Case:

$$\begin{aligned} Re_1^{-m} Nu_x &= -(x^*)^{mn} (2m)^m \left[A_3 + \frac{4}{3} Rd (3\{ 1 + (\theta_{tr} - 1)\theta(a) \} - 2) \right] \theta'(a) \\ &\quad (21) \end{aligned}$$

Solution methodology

Equations (11)–(14) along with condition Eq. (15) are numerically solved by the Bvp4c technique in MATLAB software. The Bvp4c package (inbuilt function) is an approach to handle ordinary differential equations of boundary value problems. The finite difference approach which implements the three-stage Lobatto (IIIa) formula is employed in this package; the solution can be reached by supplying an initial guess at an initial mesh point and then adjusting the step size to obtain the desired precision. Meanwhile, it is essential to reduce these boundary value problems to a system of first-order ordinary differential equations to solve them. An appropriate finite value of $\eta \rightarrow \infty$ is determined by considering values of the parameters, such that $\eta = 2$ to $\eta = 6$. Fixed values of physical parameters are taken as $a = 0.01$, $Rd = 0.5$,

Table 2 Findings of $f''(a)$ are validated at $a = 0.001$ using a range of values of n and omitting all other variables as follows

<i>n</i>	Agarwal et al. [5]	Chen and Kubler [38]	Current results
0.2	3.996×10^6	4.0×10^6	4.00×10^6
0.4	1.499×10^6	1.5×10^6	1.50×10^6
0.6	6.702×10^5	6.70×10^5	6.72×10^5
0.8	2.962×10^5	2.949×10^5	3.02×10^5
1	1.363×10^5	1.352×10^5	1.43×10^5
1.2	7.156×10^4	6.93×10^4	7.62×10^4
1.4	4.27×10^4	4.01×10^4	4.62×10^4
1.6	2.87×10^4	2.58×10^4	3.16×10^4

$\theta_{tr} = 1.5$, $Pr = 6.8$, $\phi = 0.01$ at end of the needle (i.e., $x^* = 1$), respectively.

Eventually, it is essential to determine the accuracy and reliability of the computational process employed here before studying an in-depth case study and discussing current findings. This is achieved by comparing the obtained results with the assumptions for limiting cases discovered in the existing literature. The outcomes of $f''(a)$ are in noteworthy agreement with the existing works of Agarwal et al. [5] and Chen and Kubler [38] which is displayed in Table 2.

Results and discussions

The significant outcomes of the current investigation are discussed in this section. To address the aforementioned question, the crucial role of pertinent parameters on flow profiles such as temperature and velocity is analyzed through graphical representations Figs. 4a and 5b. In addition, the value of η ranges fixed from a to ∞ where $a \neq 0$. Furthermore, the regression model was estimated using these findings. The overview of this section is included through the flow chart in Fig. 2.

Fig. 2 Outline of the results and discussion

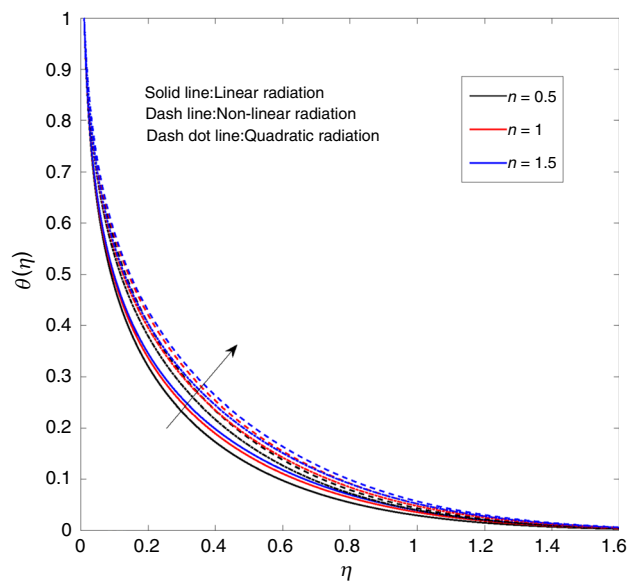
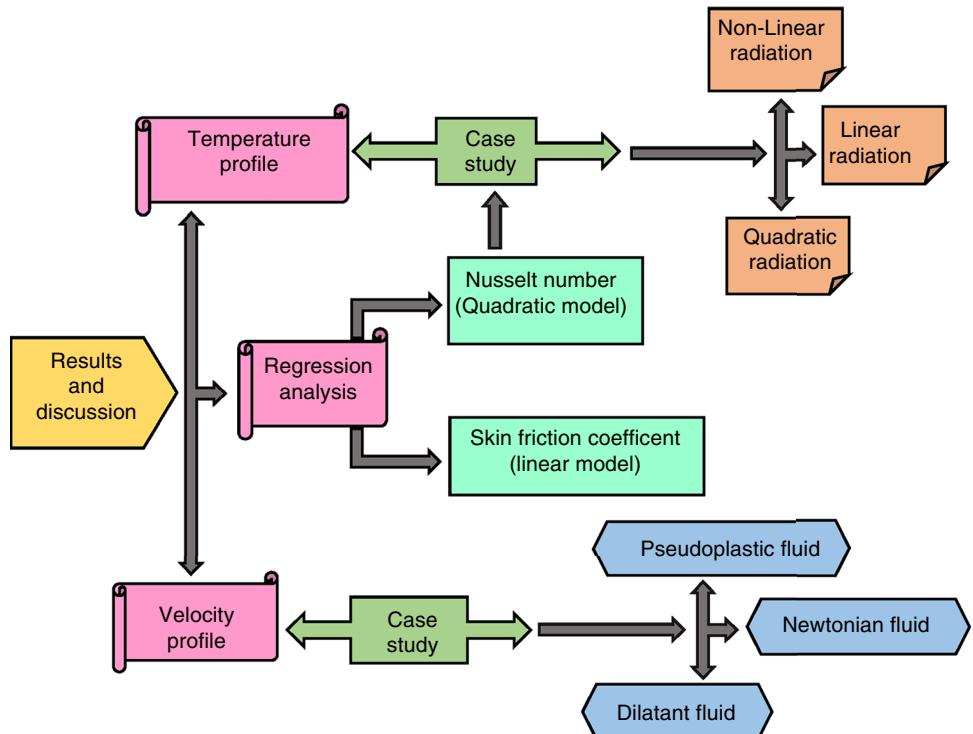


Fig. 3 Temperature profile θ for distinct values of n for three cases of radiation

Radiation case study on temperature profiles

Numerical solutions have been calculated for three cases of linear, nonlinear, and quadratic radiation. The temperature distribution (θ) is enhanced for higher values of n in Fig. 3. The temperature profile for distinct values of a , Rd , θ_{tr} and ϕ is illustrated in Fig. 4a–d for three cases of radiation.

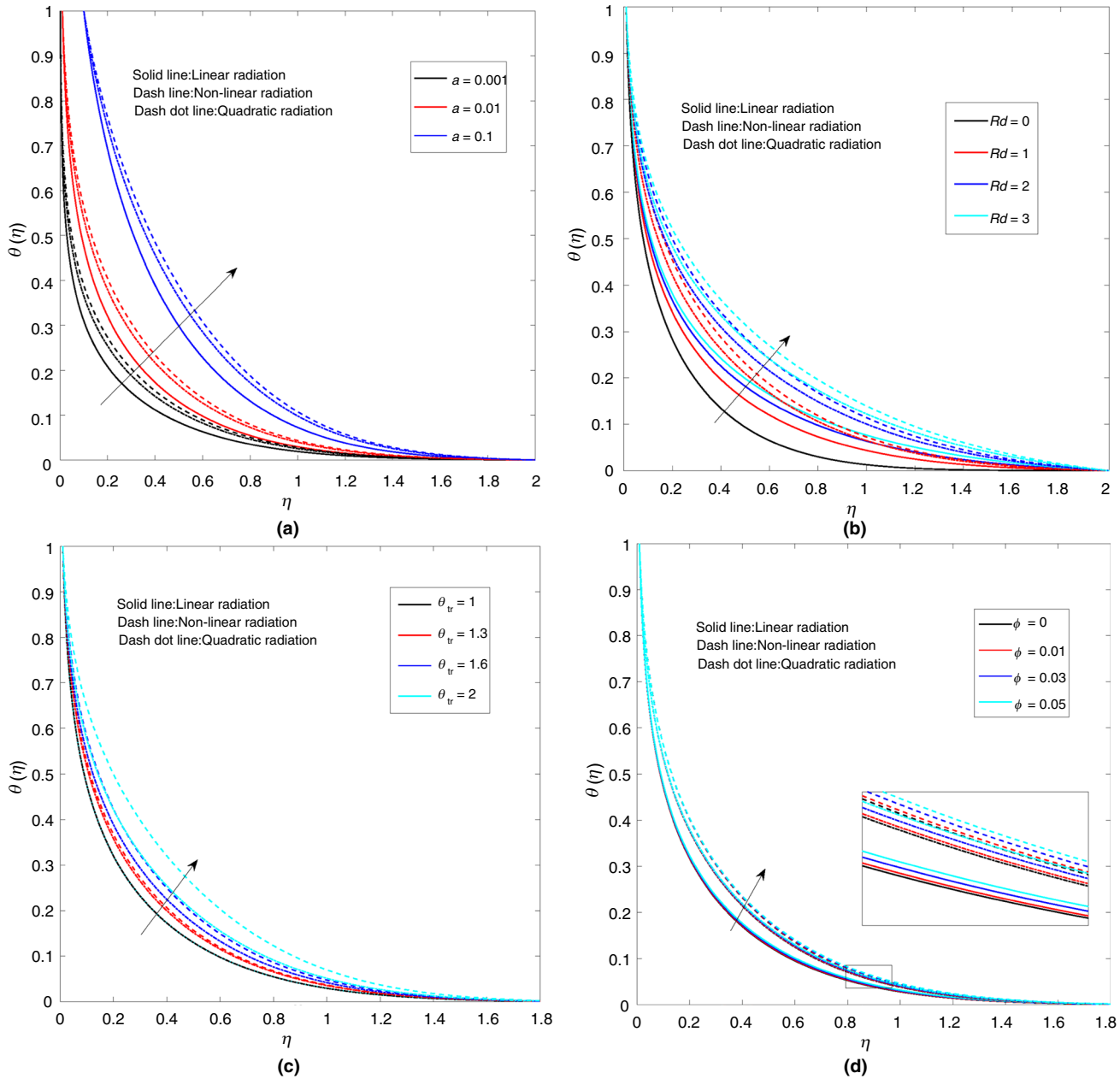


Fig. 4 Temperature profile θ for distinct values of **a**, **b** Rd , **c** θ_{tr} , **d** ϕ for three cases of radiation

Temperature profile (θ) enhanced for the variation of a , Rd , θ_{tr} , and ϕ values.

The temperature profile (θ) upsurged for the slight changes in thin needle thickness a which is displayed in Fig. 4a. These results are in noticeable agreement with recent works of Agarwal et al. [5]. The performance of the nonlinear radiation case of θ is more intense than quadratic radiation, followed by linear radiation. Therefore, using nonlinear thermal radiation is more practicable for heating/cooling processes where the temperature variation is extremely

high including photochemical reactors, rocket engines, nuclear power plants, satellites and spacecraft, cooling systems, and thermal energy storage.

The temperature profile (θ) enhanced for increasing Rd parameter in Fig. 4b. Physically, enhancing the Rd value leads to generate more thermal energy to the flow field which raises the θ in Fig. 4b. Transmission of this thermal energy into the muscles and tissues by friction below the skin destroys tumor cells by directly causing damage to their DNA (radiation therapy).

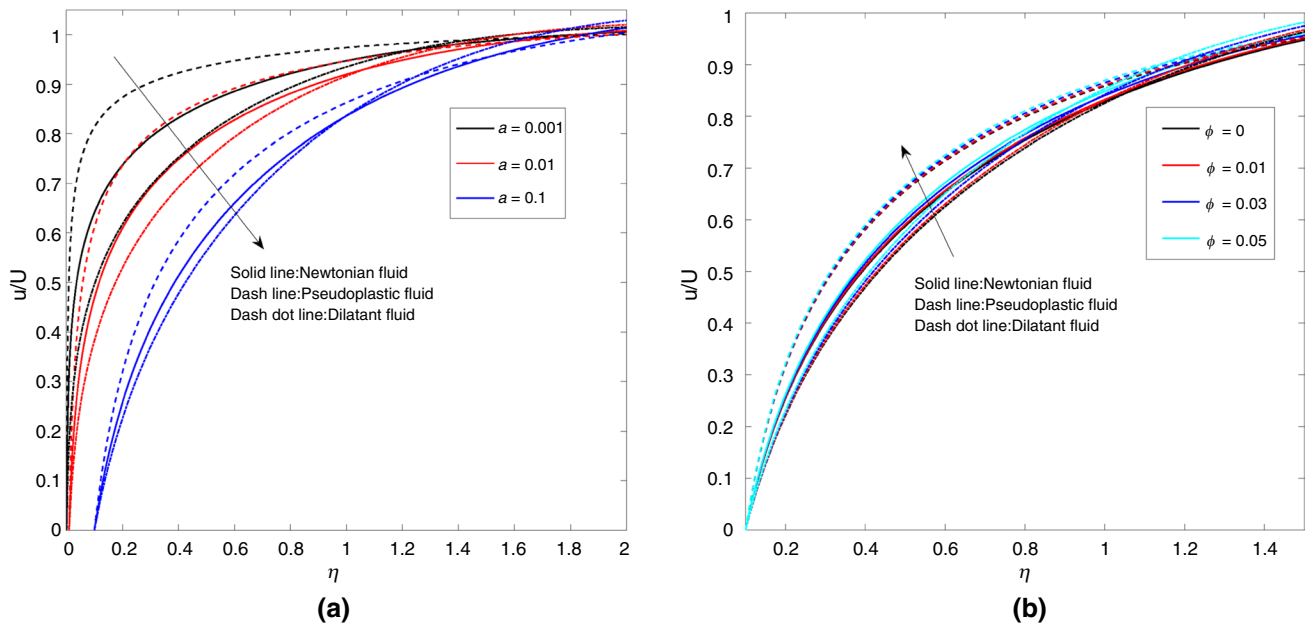


Fig. 5 Velocity profile $\frac{u}{U}$ for distinct values of **a**, **b** ϕ for three cases of power-law index (n)

Similarly, higher values of θ_{tr} enhance the surface temperature, which transfers more heat to the fluid. Consequently, θ is enhanced in Fig. 4c. Moreover, the case of nonlinear and quadratic radiation becomes the linear case, when the value of $\theta_{tr} \rightarrow 1$. This result shows good quantitative agreement with the recent work of Mahanthesh et al. [21].

The quadratic radiation case's performance is superior to the linear case but not to the nonlinear one. However, it is more practicable to employ quadratic thermal radiation when the density temperature variation is high, including solar collectors, astrophysical flows, gas production, electricity generation, and so on. From Fig. 4d, increasing TiO_2 volume fraction ϕ enhances the thermal conductivity more compared to a base fluid which upsurges the temperature profiles (θ).

Fluid case study on velocity profiles

Radiation has a minor influence on the velocity profile. Therefore, the case study of radiation is neglected and the linear case is only considered in this section. Velocity profile for distinct values of a and ϕ for three cases of power-law index n is illustrated in Fig. 5a, b. The velocity profile diminishes for higher values of a , and the reverse trend is noticed for ϕ in all cases.

By enlarging the needle size (a), more surface area comes into touch with the fluid particles, generating drag force and reducing the fluid motion, thereby raising the thermal resistance. Consequently, velocity diminished in Fig. 5a. This result shows good quantitative agreement with the recent work of Agarwal et al. [5]. The case of the pseudoplastic fluid plays a dominant role compared to the other two fluid cases because it has less apparent viscosity. A slight change in TiO_2 volume fraction ϕ values enhances the velocity profile ($\frac{u}{U}$). These results are in excellent agreement with the recent works of Hayat et al. [39]. These titanium dioxide nanoparticles are utilized as an enhancing agent in radiation therapy and computed tomography imaging (CT) process [26]. In addition, ionizing radiation targets tumors and damages tumor cells' DNA, causing the cells to die. Moreover, the Newtonian fluid performance is superior to the dilatant fluid but not to the pseudo-plastic fluid.

Regression analysis

Regression analysis is extremely important in understanding how a specific value of the dependent variable fluctuates as a result of variation in one independent variable while the rest of the variables remain constant. It is employed in numerous fields, such as forecasting, industries, and prediction. Consequently, regression model is incorporated to

evaluate the efficiency of relevant parameters on the frictional coefficient ($C_f_{est} = \log(\text{Re}_x^m C_f)$) and heat transmission rate ($Nu_{est} = \log(\text{Re}_l^{-m} Nu_x)$).

The approximation multiple linear regression models for C_f_{est} are expressed as follows [40, 41],

$$C_f_{est} = \alpha_0 + \alpha_1 a + \alpha_2 n + \alpha_3 \phi \quad (22)$$

where $\alpha_0, \alpha_1, \alpha_2, \alpha_3$ are the regression coefficients of pertinent parameters in Eq. (22).

The basic linear regression method can be utilized to estimate physical quantities with an acceptable degree of accuracy for numerous practical scenarios. However, if the goal is to obtain results that are more accurate than those of linear regression, the quadratic regression analysis is carried out.

Linear radiation case

The approximation multiple quadratic regression models for Nu_{est} are expressed as follows [21, 41, 42],

Table 3 Numerical estimation of C_f_{est} for regression coefficients and error bounds

	R^2	0.9731					
	Adjusted R^2	0.9711					
	F	494.6162					
Models	Coefficients	Std Err	LCL	UCL	t Stat	p value	Result
Intercept	1.0856	0.0551	0.9744	1.1969	19.7084	< 0.05	Significant
a	-2.8547	0.0964	-3.0494	-2.6601	-29.6203	< 0.05	Significant
n	1.1726	0.0482	1.0753	1.2700	24.3344	< 0.05	Significant
ϕ	-2.1059	0.5564	-3.2296	-0.9821	-3.7846	< 0.05	Significant

Table 4 Numerical estimation of Nu_{est} in the case of linear radiation for regression coefficients and error bounds

	R^2	0.9975					
	Adjusted R^2	0.9973					
	F	4,486.8616					
Models	Coefficients	Std err	LCL	UCL	t Stat	p value	Result
Intercept	1.7077	0.0178	1.6719	1.7436	95.8877	< 0.05	Significant
Rd	0.5126	0.0104	0.4917	0.5335	49.3849	< 0.05	Significant
ϕ	1.1230	0.4609	0.1946	2.0514	2.4364	< 0.05	Significant
$Rd \times \phi$	-0.1882	0.1486	-0.4875	0.1110	-1.2668	> 0.05	Insignificant
Rd^2	-0.0419	0.0017	-0.0453	-0.0386	-25.2420	< 0.05	Significant

Table 5 Numerical estimation of Nu_{est} in the case of nonlinear radiation for regression coefficients and error bounds

	R^2	0.9986					
	Adjusted R^2	0.9985					
	F	10,210.4288					
Models	Coefficients	Std Err	LCL	UCL	t Stat	p value	Result
Intercept	0.6205	0.0765	0.4690	0.7720	8.1138	< 0.05	Significant
Rd	0.4870	0.0103	0.4666	0.5074	47.2577	< 0.05	Significant
ϕ	1.0715	0.7937	-0.5005	2.6436	1.3500	> 0.05	Insignificant
θ_{tr}	1.1155	0.0900	0.9372	1.2937	12.3941	< 0.05	Significant
$Rd \times \phi$	-0.0929	0.0917	-0.2744	0.0886	-1.0139	> 0.05	Insignificant
$\phi \times \theta_{tr}$	-0.3108	0.4583	-1.2184	0.5969	-0.6781	> 0.05	Insignificant
$Rd \times \theta_{tr}$	0.0634	0.0046	0.0543	0.0724	13.8258	< 0.05	Significant
Rd^2	-0.0475	0.0011	-0.0497	-0.0453	-43.3620	< 0.05	Significant
θ_{tr}^2	-0.0797	0.0274	-0.1339	-0.0254	-2.9090	< 0.05	Significant

$$Nu_{\text{est}} = \lambda_0 + \lambda_1 Rd + \lambda_2 \phi + \lambda_3 Rd\phi + \lambda_4 Rd^2 \quad (23)$$

where $\lambda_0, \lambda_1, \lambda_2, \lambda_3, \lambda_4$ are the regression coefficients of pertinent parameters in Eq. (23).

Nonlinear radiation and quadratic radiation case

The approximation multiple quadratic regression models for Nu_{est} for the nonlinear and quadratic radiation cases are expressed as follows [21, 40, 42],

$$Nu_{\text{est}} = \beta_0 + \beta_1 Rd + \beta_2 \phi + \beta_3 \theta_{\text{tr}} + \beta_4 Rd\phi + \beta_5 \phi \theta_{\text{tr}} + \beta_6 Rd\theta_{\text{tr}} + \beta_7 Rd^2 + \beta_8 \theta_{\text{tr}}^2 \quad (24)$$

where $\beta_0, \beta_1, \beta_2, \dots, \beta_8$ are the regression coefficients of pertinent parameters in Eq. (24).

In order to calculate the regression coefficients in Eqs. (22)–(24), the distinct combinations of 50–125 sets of values of a, n, ϕ and $Rd, \theta_{\text{tr}}, \phi$ are utilized to estimate the frictional drag coefficient (Cf_{est}) and thermal transmission rate (Nu_{est}) from Eq. (18)–(21).

The coefficients have been estimated from these data collections and displayed in Tables 3–6. The t-statistics test is also performed, which is a useful tool for determining if a coefficient is substantially different from zero. The LCL and UCL denote the lower and upper limit of the 95% confidence interval. A low p value ($p < 0.05$) in Tables 3–6 indicates a significant improvement in the model's fit. All terms are significant except the term with factor ϕ .

The R^2 value represents the coefficient of determination which ranges between 0 and 1 and contributes to the

estimation of the regression model as a whole. It helps to measure the goodness of fit. Similarly, when comparing models with distinct values of independent variables, the adjusted R^2 might be helpful. The values of R^2 and adjusted R^2 are closer to 1 in tables 3–6 which indicates the high accuracy of the model. The precision of the estimated regression model (for the selected sample) was determined through Fig. 6a–d. The results show a satisfactory agreement between the actual and estimated values of Cf_{est} in Fig. 6a and Nu_{est} in Fig. 6b–d. The quadratic regression model shows more accurate results compared to the linear regression model.

From table 3, the Cf_{est} has been adversely influenced by the parameters a and ϕ , as seen in table 3 and n has a positive influence on the same. While Nu_{est} is improved by the parameter of Rd, ϕ for all radiation scenarios, Rd^2 behaves oppositely. The case of linear radiation plays the dominant role compared to the other two radiation cases. The factor of $Rd \times \theta_{\text{tr}}$ has a positive effect on Nu_{est} but $Rd \times \phi$, and $\phi \times \theta_{\text{tr}}$ behaves in a reverse manner in both the nonlinear and quadratic radiation cases. The quadratic term of Rd and θ_{tr} has a negative influence on Nu_{est} . The case of nonlinear radiation has a larger influence compared to the quadratic radiation case.

These results might be useful in various industrial approaches such as astrophysical flows, electrical power generation, melt spinning techniques for cooling liquid, geothermal extractions, space vehicles, nuclear energy plants, and solar systems. Especially, it is essential for testing automobiles, weather analysis, and prediction.

Table 6 Numerical estimation of Nu_{est} in the case quadratic radiation for regression coefficients and error bounds

	R^2	0.9985						
	Adjusted R^2	0.9984						
	F	9,937.9319						
Models	Coefficients	Std Err	LCL	UCL	t Stat	<i>p</i> value	Result	
Intercept	0.6919	0.0675	0.5582	0.8256	10.2499	< 0.05	Significant	
Rd	0.4908	0.0091	0.4727	0.5088	53.9515	< 0.05	Significant	
ϕ	1.0230	0.7006	-0.3647	2.4106	1.4601	> 0.05	Insignificant	
θ_{tr}	1.2323	0.0794	1.0750	1.3897	15.5128	< 0.05	Significant	
$Rd \times \phi$	-0.1063	0.0809	-0.2665	0.0540	-1.3135	> 0.05	Insignificant	
$\phi \times \theta_{\text{tr}}$	-0.2255	0.4045	-1.0267	0.5756	-0.5576	> 0.05	Insignificant	
$Rd \times \theta_{\text{tr}}$	0.0449	0.0040	0.0369	0.0530	11.1110	< 0.05	Significant	
Rd^2	-0.0447	0.0010	-0.0467	-0.0428	-46.2722	< 0.05	Significant	
θ_{tr}^2	-0.2258	0.0242	-0.2737	-0.1779	-9.3413	< 0.05	Significant	

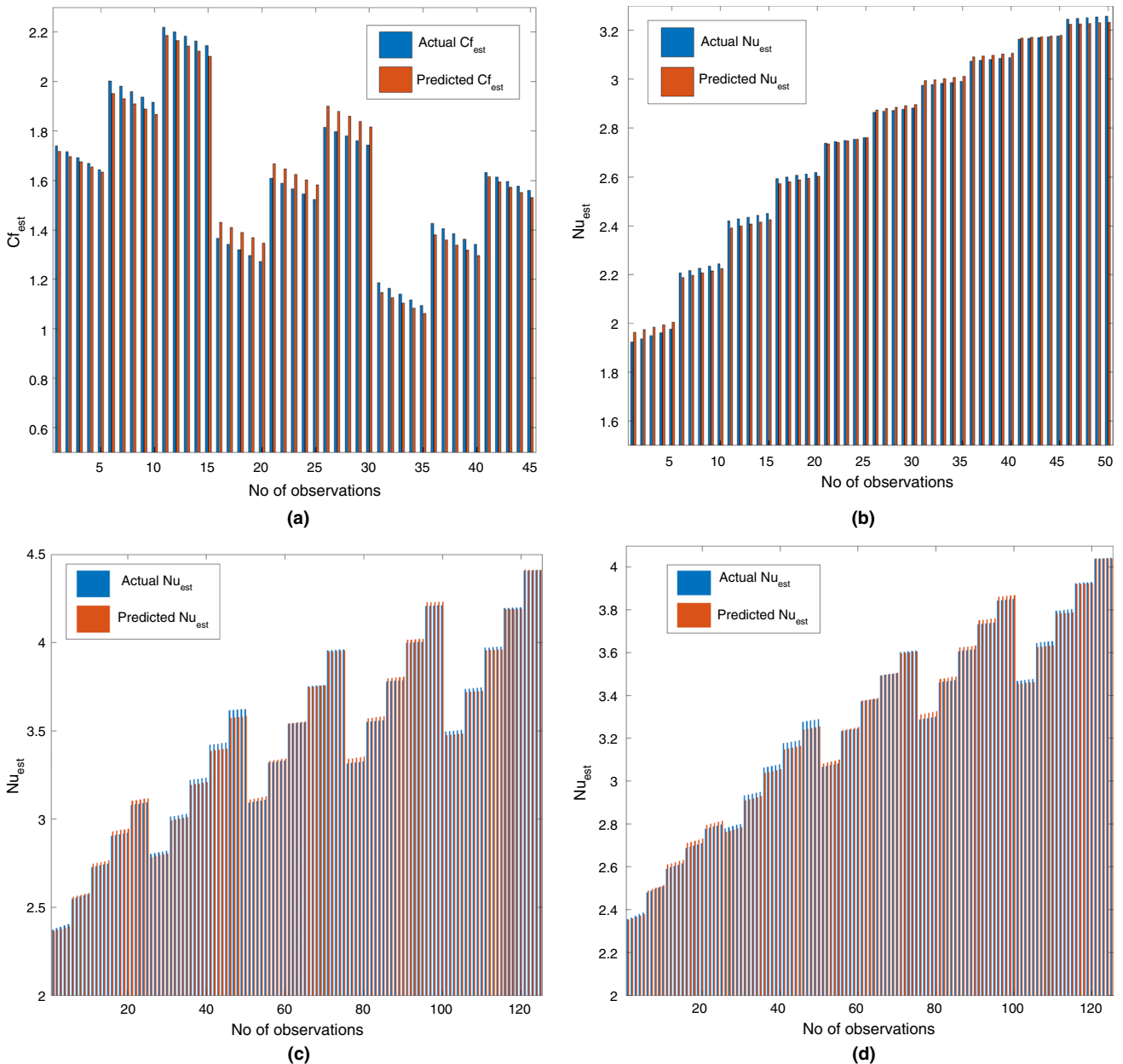


Fig. 6 Comparing actual versus predicted values of **a** Cf_{est} **b** Nu_{est} in linear radiation case **c** Nu_{est} in nonlinear radiation case **d** Nu_{est} in quadratic radiation case

Conclusions

We have examined the comparative study of radiation on the power-law nanofluid flow over a thin needle. Water-based TiO_2 nanofluid has been incorporated. The significance of relevant parameters is discussed clearly in the previous section of the current investigation, which has numerous applications across various industrial fields. Additionally,

multiple linear and quadratic regression analysis has been used to quantitatively examine how pertinent parameters affect the surface drag coefficient and the rate of heat transmission. The main conclusions are enumerated here.

- Temperature profile upsurged for higher values of dimensionless needle size(a), radiation parameter (Rd), and TiO_2 volume fraction (ϕ).

- The performance of the nonlinear radiation case of θ is more intense than the quadratic case, followed by the linear case.
- Velocity profile diminished by enhancing a parameter and reverse trend noticed for ϕ value. The case of pseudoplastic fluid plays a dominant role on $\frac{u}{U}$ compared to a Newtonian fluid, followed by dilatant fluid.
- The performance of ϕ has a negative influence on the drag coefficient, but it behaved oppositely on the heat transmission rate.
- The quadratic regression model shows more accurate results compared to the linear regression model.

The outcomes of this investigation may help to get a better theoretical understanding of various scientific research and biomedical applications, especially in the treatment of tumors, sterilization of medical instruments, drug delivery systems, and cancer treatment.

Author Contributions PS involved in investigation (equal), methodology (equal), validation (equal), visualization (equal) & writing—original draft (equal); PN took part in conceptualization (lead), methodology (equal), supervision (lead), writing—review & editing (equal).

Data Availability Statement Data sharing is not applicable to this article as no new data were created or analyzed in this study.

Declarations

Conflict of interest No conflicts of interest have been disclosed by the authors

Future scope There are numerous possibilities for further research on the current study. It can be extended by considering various kinds of nanoparticles, the shapes, and sizes of nanoparticles, different thermophysical properties of nanofluids, and the irreversibility analysis. Also, it is expected that this work will stimulate experimental research to explore technical applications to sustainable fuel cell technologies, biosensors, manufacturing of drugs, beauty products, petrochemical products, biochemicals, and hygiene product.

References

- Bush M. Applications in non-Newtonian fluid mechanics. In: Viscous flow applications. Springer; 1989; p. 134–60.
- Hoyt J. Some applications of non-newtonian fluid flow. In: Rheology Series. vol. 8. Elsevier; 1999. p. 797–826.
- Bahmani A, Kargarsharifabad H. Laminar natural convection of power-law fluids over a horizontal heated flat plate. *Heat Trans Asian Res*. 2019;48(3):1044–66.
- Parveez M, Harmain G, Dhiman A, Khan J. Flow characteristics of power-law fluid around circular cylinder. In: Recent advances in mechanical engineering: select proceedings of CAMSE 2021. Springer; 2022. p. 225–36.
- Agarwal M, Chhabra R, Eswaran V. Laminar momentum and thermal boundary layers of power-law fluids over a slender cylinder. *Chem Eng Sci*. 2002;57(8):1331–41.
- Gajbhiye S, Warke A, Katta R. Heat transfer and fluid flow analysis of non-Newtonian fluid in a microchannel with electromagneto hydrodynamics and thermal radiation. *Heat Trans*. 2022;51(2):1601–21.
- Naveen P, RamReddy C. Quadratic convection in a power-law fluid with activation energy and suction/injection effects. *Int J Ambient Energy*. 2023;44(1):822–34.
- Choi SU, Eastman JA. Enhancing thermal conductivity of fluids with nanoparticles. Argonne National Lab. (ANL), Argonne; 1995.
- Ganvir R, Walke P, Kriplani V. Heat transfer characteristics in nanofluid—a review. *Renew Sustain Energy Rev*. 2017;75:451–60.
- Rashidi S, Mahian O, Languri EM. Applications of nanofluids in condensing and evaporating systems: a review. *J Therm Anal Calorim*. 2018;131:2027–39.
- Sayee MA, Podder A, Mishra S, Afikuzzaman M, Alam MM. Computational modeling of unsteady MHD nanofluid over a cylinder using gyrotactic microorganisms. *J Therm Anal Calorim*. 2023;148(21):11855–70.
- Jusoh R, Nazar R, Pop I. Three-dimensional flow of a nanofluid over a permeable stretching/shrinking surface with velocity slip: a revised model. *Phys Fluids*. 2018;30(3).
- Firoozzadeh M, Shafiee M. Thermodynamic analysis on using titanium oxide/oil nanofluid integrated with porous medium in an evacuated tube solar water heater. *J Therm Anal Calorim*. 2023;1–14.
- Sridhar V, Ramesh K. Peristaltic activity of thermally radiative magneto-nanofluid with electroosmosis and entropy analysis. *Heat Trans*. 2022;51(2):1668–90.
- Sheikhpor M, Arabi M, Kasaeian A, Rokn Rabeı A, Taherian Z. Role of nanofluids in drug delivery and biomedical technology: methods and applications. *Nanotech Sci Appl*. 2020;47–59.
- Liu L, Miao P, Xu Y, Tian Z, Zou Z, Li G. Study of Pt/TiO₂ nanocomposite for cancer-cell treatment. *J Photochem Photobiol B Biol*. 2010;98(3):207–10.
- Çeşmeli S, Biray AC. Application of titanium dioxide (TiO₂) nanoparticles in cancer therapies. *J Drug Target*. 2019;27(7):762–6.
- Shi H, Magaye R, Castranova V, Zhao J. Titanium dioxide nanoparticles: a review of current toxicological data. Part Fibre Toxi-col. 2013;10:1–33.
- Sung W, Hong TS, Poznansky MC, Paganetti H, Grassberger C. Mathematical modeling to simulate the effect of adding radiation therapy to immunotherapy and application to hepatocellular carcinoma. *Int J Radiat Oncol Biol Phys*. 2022;112(4):1055–62.
- Magyari E, Pantokratoras A. Note on the effect of thermal radiation in the linearized Rosseland approximation on the heat transfer characteristics of various boundary layer flows. *Int Commun Heat Mass Trans*. 2011;38(5):554–6.
- Mahanthesh B, Mackolil J, Radhika M, Al-Kouz W, et al. Significance of quadratic thermal radiation and quadratic convection on boundary layer two-phase flow of a dusty nanoliquid past a vertical plate. *Int Commun Heat Mass Trans*. 2021;120: 105029.
- Gajbhiye S, Warke A, Ramesh K. Analysis of energy and momentum transport for Casson nanofluid in a microchannel with radiation and chemical reaction effects. *Waves Random Complex Media*. 2022;1–29.
- Mahabaleshwar U, Nagaraju K, Vinay Kumar P, Azese MN. Effect of radiation on thermosolutal Marangoni convection in a porous medium with chemical reaction and heat source/sink. *Phys Fluids*. 2020;32(11).
- Yaseen M, Garia R, Rawat SK, Kumar M. Hybrid nanofluid flow over a vertical flat plate with Marangoni convection in the

- presence of quadratic thermal radiation and exponential heat source. *Int J Ambient Energy.* 2023;44(1):527–41.
- 25. Makinde O, Animasaun I. Bioconvection in MHD nanofluid flow with nonlinear thermal radiation and quartic autocatalysis chemical reaction past an upper surface of a paraboloid of revolution. *Int J Therm Sci.* 2016;109:159–71.
 - 26. Smith L, Kuncic Z, Ostrikov K, Kumar S. Nanoparticles in cancer imaging and therapy. *J Nanomater.* 2012;2012:1–7.
 - 27. Lee LL. Boundary layer over a thin needle. *Phys Fluids.* 1967;4(10):820–2.
 - 28. Hassan M, Rizwan M. Mathematical modeling for experimental data to investigate the convective heat transfer in non-Newtonian nanofluid's flow over a thin needle. *ZAMM J Appl Math Mech.* 2023;e202200344.
 - 29. Ahmad R, Mustafa M, Hina S. Buongiorno's model for fluid flow around a moving thin needle in a flowing nanofluid: a numerical study. *Chin J Phys.* 2017;55(4):1264–74.
 - 30. Souayah B, Reddy MG, Sreenivasulu P, Poornima T, Rahimi-Gorji M, Alarifi IM. Comparative analysis on non-linear radiative heat transfer on MHD Casson nanofluid past a thin needle. *J Mol Liq.* 2019;284:163–74.
 - 31. Jyothi A, Kumar RN, Gowda RP, Prasannakumara B. Significance of Stefan blowing effect on flow and heat transfer of Casson nanofluid over a moving thin needle. *Commun Theoret Phys.* 2021;73(9): 095005.
 - 32. Tiwari RK, Das MK. Heat transfer augmentation in a two-sided lid-driven differentially heated square cavity utilizing nanofluids. *Int J Heat Mass Trans.* 2007;50(9):2002–18.
 - 33. Patil MB, Shobha K, Bhattacharyya S, Said Z. Soret and Dufour effects in the flow of Casson nanofluid in a vertical channel with thermal radiation: entropy analysis. *J Therm Anal Calorim.* 2023;148(7):2857–67.
 - 34. Makinde O, Animasaun I. Thermophoresis and Brownian motion effects on MHD bioconvection of nanofluid with non-linear thermal radiation and quartic chemical reaction past an upper horizontal surface of a paraboloid of revolution. *J Mol Liq.* 2016;221:733–43.
 - 35. Mustafa M, Mushtaq A, Hayat T, Alsaedi A. Model to study the non-linear radiation heat transfer in the stagnation-point flow of power-law fluid. *Int J Numer Methods Heat Fluid Flow.* 2015;25(5):1107–19.
 - 36. Permanasari AA, Kuncara BS, Puspitasari P, Sukarni S, Ginta TL, Irdianto W. Convective heat transfer characteristics of TiO₂-EG nanofluid as coolant fluid in heat exchanger. In: AIP conference proceedings. vol. 2120. AIP Publishing; 2019.
 - 37. Riahi A, Ben-Cheikh N, Campo A. Water-based nanofluids for natural convection cooling of a pair of symmetrical heated blocks placed inside a rectangular enclosure of aspect ratio two. *Int J Therm Environ Eng.* 2018;16(1):1–10.
 - 38. Chen J, Kubler E. Non-Newtonian flow along needles. *Phys Fluids.* 1978;21(5):749–51.
 - 39. Hayat T, Khan MI, Farooq M, Yasmeen T, Alsaedi A. Water-carbon nanofluid flow with variable heat flux by a thin needle. *J Mol Liq.* 2016;224:786–91.
 - 40. Sahoo A, Nandkeolyar R. Entropy generation in convective radiative flow of a Casson nanofluid in non-Darcy porous medium with Hall current and activation energy: the multiple regression model. *Appl Math Comput.* 2021;402: 125923.
 - 41. Siegel AF, Wagner MR. Chapter 12—multiple regression: predicting one variable from several others. In: Siegel AF, Wagner MR, editors. Practical business statistics (Eighth Edition). eighth edition ed. Academic Press; 2022. p. 371–431.
 - 42. Carroll JD, Green PE. Chapter 6—applying the tools to multivariate data. In: Carroll JD, Green PE, editors. Mathematical tools for applied multivariate analysis. San Diego: Academic Press; 1997. p. 259–94.

Publisher's Note Springer Nature remains neutral with regard to jurisdictional claims in published maps and institutional affiliations.

Springer Nature or its licensor (e.g. a society or other partner) holds exclusive rights to this article under a publishing agreement with the author(s) or other rightsholder(s); author self-archiving of the accepted manuscript version of this article is solely governed by the terms of such publishing agreement and applicable law.